HHS Public Access

Author manuscript

J Hand Surg Am. Author manuscript; available in PMC 2020 September 01.

Published in final edited form as:

J Hand Surg Am. 2019 September ; 44(9): 751–761. doi:10.1016/j.jhsa.2019.05.007.

The Biomechanical Basis of the Claw Finger Deformity: A Computational Simulation Study

Benjamin I Binder-Markey, DPT, PhD[a,b,c,d], **Julius P.A. Dewald, PhD**[a,b,c], **Wendy M Murray, PhD**[a,b,c,d,e]

[a)]Dept. of Biomedical Engineering, Northwestern University, 2145 Sheridan Road Evanston, IL 60208 USA

[b)]Dept. of Physical Therapy and Human Movement Sciences, Northwestern University, 645 N. Michigan Ave, Suite 1100, Chicago, IL 60611 USA

[c)]Dept. of Physical Medicine and Rehabilitation Science, Northwestern University, 710 North Lake Shore Drive Chicago, IL 60611 USA

[d)]Shirley Ryan AbilityLab, 355 E Erie St, Chicago, IL 60611 USA

[e)]Research Service, Edward Hines Jr., VA Hospital, 5000 5th Ave, Hines, IL 60141 USA

Abstract

Purpose—Claw finger deformity occurs during attempted finger extension in patients whose intrinsic finger muscles are weakened or paralyzed by neural impairments. The deformity is generally not acutely present following intrinsic muscle palsy. The delayed onset, with severity progressing over time, suggests that soft tissue changes that effect the passive biomechanics of the hand, exacerbate and advance the deformity. Clinical interventions may be more effective if such secondary biomechanical changes are effectively addressed. Using a computational model, we simulated these altered soft tissue biomechanical properties on coordinated finger extension to quantify their effects.

Methods—To evaluate the effects of maladaptive changes in soft tissue biomechanical properties on the development and progression of the claw finger deformity following intrinsic muscle palsy, we completed 45 biomechanical simulations of cyclic index finger flexion and extension, varying muscle excitation level, clinically relevant biomechanical factors, and wrist position. We evaluated to what extent (i) increased joint laxity, (ii) decreased mechanical advantage of the extensors about the PIP joint, and (iii) shortening of the flexor muscles contributed to the development of claw finger deformity in an “intrinsic-minus” hand model.

Results—Of the mechanisms studied, shortening (or contracture), of the extrinsic finger flexors was the factor most associated with the development of claw finger deformity in simulation.

Corresponding Author: Wendy M. Murray, PhD, Shirley Ryan AbilityLab, 355 E. Erie St., 20th Floor, Chicago, IL 60611, w-murray@northwestern.edu.

Conclusions—Our simulations suggest adaptive shortening of the extrinsic finger flexors is required for the development of claw finger deformity. Increased joint laxity and decreased extensor mechanical advantage only contributed to the severity of the deformity in simulation when shortening of the flexor muscles was present.

Clinical Relevance—In both the acute and chronic stages of intrinsic finger paralysis, maintaining extrinsic finger flexor length should be an area of focus in rehabilitation, to prevent the formation of the claw finger deformity and achieve optimal outcomes after surgical interventions.

Keywords

biomechanics; claw-finger deformity; computational musculoskeletal modeling; finger; hand

1. INTRODUCTION

The claw finger deformity is present in many patients in whom intrinsic finger muscles are weakened or paralyzed due to neural impairments. During healthy finger extension, the intrinsic finger muscles act synergistically with the extrinsic finger muscles to prevent metacarpophalangeal (MCP) hyperextension and, via the extensor mechanism, couple proximal and distal interphalangeal joint extension.[1–7] With weakened or paralyzed intrinsic muscles, the claw deformity occurs during attempted finger extension; instead, the MCP joints hyperextend while the PIP and DIP joints concomitantly flex.[6,7] This dyscoordination impedes finger extension and limits the ability to grasp objects and functionally use the hand.

The claw finger deformity is not present immediately following intrinsic muscle palsy.[8,9] Rather, the onset is delayed and the severity may progress over time. As a result, changes in soft tissue biomechanical properties are postulated to exacerbate the loss of intrinsic muscle function.[9] For example, individuals who have lax MCP joints may develop the claw finger deformity earlier and with greater severity than those with stiffer fingers.[8–10] Additionally, as hand use decreases, maladaptive changes are thought to advance the deformity. For example, as the fingers remain in a flexed resting position for extended periods, the extensor mechanism is thought to stretch.[9] Specifically, it is postulated that the central slip and the dorsal hood of the extensor mechanism elongate,[8,9] resulting in volar translation of the lateral slips during PIP joint flexion.[9] Volar translation of the lateral slips decreases the mechanical advantage of the extensor mechanism about the PIP joint and, therefore, decreases the capacity of the extensor muscles to extend the PIP joint. The flexed, resting hand position is also postulated to cause contracture (or adaptive shortening) of the extrinsic finger flexor muscles, similar to muscle shortening following limb immobilization.[11,12] Adaptive shortening of the extrinsic flexor muscles would add to the severity of the deformity because it would result in larger passive resistive forces about the finger joints.[6,9]

Clinical interventions to mitigate the claw finger deformity focus on replacing function of the paralyzed intrinsic finger muscles. For example, the synergistic intrinsic muscle activity that prevents MCP hyperextension during finger extension is emulated clinically either via orthoses[13–15] or surgical procedures that include bone blocks,[16] tenodeses, [17–19] or volar

plate capsulodesis.[10] Additionally, numerous active tendon transfers have been developed to improve coordination of distal finger joint extension following loss of intrinsic muscle function.[7,8] In these procedures, the paths of functioning muscle-tendon units[6,17,20–22] are attached distally to the dorsal aspect of the fingers, after first being routed on the volar side of the MCP joint, mimicking the intrinsic muscles' actions at the finger joints.

While clinical interventions that aim to find substitutes for active intrinsic muscle function are essential, clinical outcomes may also benefit from interventions that more directly address the secondary biomechanical changes that contribute to the development of the deficit. Because these secondary changes and their effects appear to be neither fully understood nor easily quantified, such treatment strategies are more difficult to define. The objective of this study was to simulate the effects of changes to the soft tissue biomechanical properties on coordinated finger extension using a computational model. We designed a series of biomechanical simulations to evaluate the contributions of (i) increased joint laxity, (ii) decreased mechanical advantage of the extensors about the PIP joint, and (iii) shortening of the flexor muscles on the development of claw finger deformity in an "intrinsic-minus" hand model. Because clinical observations indicate that increased joint stiffness limits the severity of the deformity[8–10] and because many successful clinical interventions focus on the prevention of MCP hyperextension,[13–19] we hypothesized that simulations that incorporated increased joint laxity would be the most likely to generate the claw finger deformity.

2. METHODS

2.1. Musculoskeletal Model

To simulate the effects of changes to the soft tissue biomechanical properties on coordinated finger extension following intrinsic muscle palsy, a previously described biomechanical model[23] was used to generate forward dynamic simulations of active finger flexion and extension (OpenSim v3.3[24]). Forward dynamic simulations involve an iterative, sequential process in which muscle excitation inputs are transformed into muscle forces via differential equations that represent the phenomena of excitation-contraction coupling and muscle contraction.[25] At each time step of the simulation, the calculated muscle forces are applied to the skeleton and joint motion is predicted via Newton's second law. A 'one-at-a-time' factorial analysis[26] was performed to evaluate to what extent (i) increased joint laxity, (ii) decreased mechanical advantage of the extensors about the PIP joint, and (iii) shortening of the flexor muscles contributed to the development of claw finger deformity. That is, we performed multiple simulations, with each simulation systematically incorporating these factors in the model at different levels of severity so that we could understand how each factor affects coordinated finger extension, first individually, and then combined.

The biomechanical model includes the radius, ulna, carpal, metacarpal, and phalangeal bones of the hand with mass and inertial properties defined to be consistent with the anthropometrics of a 50th percentile male.[23,27,28] Wrist and index finger kinematics were implemented as previously defined.[23,29] Muscle-tendon paths and force-generating properties (both active and passive) of the four extrinsic index finger muscles; flexor digitorum superficialis indicis (FDSI), flexor digitorum profundus indicis (FDPI), extensor digitorum communis indicis (EDCI), and extensor indicis proprius (EIP); were explicitly

defined within the model.[23] The net passive torques contributed by intrinsic muscles and soft tissue structures (e.g., ligaments, joint capsules, and skin) that cross the MCP, PIP, and DIP joints of the index finger were implemented into the model as three torsional spring-dampers, each independently acting about the flexion-extension axis of each joint.[23] Consistent with an "intrinsic-minus" hand,[4,9,18] active force-generating properties of the intrinsic finger muscles were excluded from the model. This model includes only the index finger because critical data (e.g., moment arms, passive joint torques) currently exist only for the index finger. Because of similarities in joint geometry, structure, and muscle actions between fingers, we expect the conclusions drawn from this index finger model may be extrapolated to the remaining fingers.

2.2. Dynamic Simulations

Using the nominal, "intrinsic-minus" hand model to mimic acute intrinsic muscle paralysis prior to any soft tissue changes, we developed forward dynamic simulations of a single cycle of index finger flexion followed by index finger extension to evaluate extension of the finger from an initial flexed position. At the end of the flexion and extension cycle, the final equilibrium position of the finger was evaluated for the presence of the claw finger deformity, defined as hyperextension (extension beyond 0 degrees) of the MCP joint and concurrent flexion of the PIP joint greater than 20 degrees.

Muscle excitation inputs were defined over a 4-second interval. For the two extrinsic flexors, the muscle excitation input was a simple "on/off" function; both muscles were turned "on" at simulation time of 1 s, and "off" at 2 s. For the two extrinsic extensors, muscle excitation initiated at 2 s, and was maintained at a constant level for the remainder of the simulation (Fig. 1). We compared the final equilibrium positions for three distinct excitation magnitudes (20%, 50%, and 100%) that replicated EMG data observed experimentally for these muscles during slow, medium, and fast movements, respectively.[30] Excitation timing was constant across all simulations. The forearm was pronated with the hand oriented horizontally so that gravity opposes wrist extension. The wrist was extended 30°, reflecting a wrist position adopted during reaching and grasping activities.[31–33] Forearm and wrist positions were held constant throughout the simulation of index finger motion. The remaining unconstrained degrees of freedom (MCP, PIP, and DIP joint angles) were simulated with time.

2.3. One-factor-at-a-time Sensitivity Analysis

We completed 27 additional forward dynamic simulations as a part of a 'one-factor-at-a-time' analysis. For a given set of simulated soft tissue biomechanical property changes, the original three simulations and analyses were repeated (see Table 1).

First, to simulate the effects of increased joint laxity, the passive joint torques in the nominal "intrinsic-minus" model (defined based on experimental data[34,35]) were uniformly scaled to three different levels, with magnitudes equal to 75%, 50%, or 25% of the nominal torques (Fig. 2). Similarly, we repeated the nominal simulations with smaller PIP extension moment arms to evaluate the effects of decreased mechanical advantage of the extrinsic index extensor muscles (Fig. 3). To do so, we reduced the diameter of the kinematic constraint that

determines the distance between the muscle-tendon path and the PIP joint center in flexed positions. Simulations were repeated at 75%, 50%, and 25% of the nominal diameter. For each of these two biomechanical factors, the range of parameter values was defined to represent substantial biomechanical changes relative to the acute “intrinsic-minus” hand.

Finally, adaptive shortening of the extrinsic index finger flexor muscles was simulated relative to the nominal “resting length” of the muscle-tendon units.[23] We define “resting length” based on the understanding that muscle-tendon actuators only generate passive forces at lengths where both the tendon is longer than its slack length (L_{ts}; the length where the tendon begins to transmit force[25]) and the muscle fibers are longer than optimal length (L_{fo}; the length of a muscle’s fibers at maximum active force and generally assumed to correspond to the onset of passive force generation[25]). Resting muscle-tendon length, $L_{mt,r}$, is defined mathematically as:

$$L_{mt,r} = L_{ts} + \cos(\alpha) L_{fo}$$

where α is the pennation angle of the muscle fibers with respect to the tendon. To simulate shortening of FDSI and FDPI, L_{ts} and L_{fo} were uniformly decreased for both muscles to either 98%, 95%, or 90% of their nominal lengths. Shortening $L_{mt,r}$ of the extrinsic flexor muscle-tendon units shifts the limb position where the muscle-tendon units generate passive forces to more flexed positions, larger decreases in $L_{mt,r}$ resulted in a more flexed resting finger position (Table 2). Decreasing $L_{mt,r}$ to 90% of nominal length drastically increased the passive resistive flexion forces and resulting torques at the MCP and PIP joints (Fig. 4), throughout the range of motion. Because the main simulation result for decreases in $L_{mt,r}$ greater than 90% of the nominal length was that index finger extension was not possible at any activation level, we did not evaluate decreases beyond 90%.

2.4. Sensitivity analysis to the combination of all factors

The sensitivity of coordinated finger extension to the combination of all factors was evaluated with all of the (i) mild (75% torque, 75% moment arm, 98% $L_{mt,r}$), (ii) moderate (50% torque, 50% moment arm, 95% $L_{mt,r}$), and (iii) severe (25% torque, 25% moment arm, 90% $L_{mt,r}$) changes combined, respectively. These 9 simulations were then repeated with the wrist flexed 30° to mimic the Andre-Thomas compensation strategy, often adopted by individuals with mild claw finger deformities to achieve finger extension.[8,9]

3. RESULTS

Within the 27 simulations for the ‘one-factor-at-a-time’ sensitivity analysis, the only biomechanical factor associated with the development of the claw finger deformity in our “intrinsic-minus” model was shortening of the extrinsic finger flexor muscles. For the 9 simulations where $L_{mt,r}$ was modified, the results indicate that the deformity is sensitive to both impairment level and muscle excitation (Fig 5). Specifically, mild changes in resting lengths (98% $L_{mt,r}$) produced the claw finger deformity with 20% excitation. However, coordinated finger extension was achieved with higher excitations (cf., Fig. 5, top row). With moderate length changes (95% $L_{mt,r}$), coordinated finger extension was not achievable at

any excitation level (cf., Fig. 5, middle row). At the 20% excitation level, the extensor muscle forces produced were not large enough to overcome the increased passive resistance at the MCP joint that resulted from the shortened flexors (Fig. 4), causing MCP flexion in equilibrium. Increased excitation levels (and the resulting larger extensor muscle forces) produced the claw finger deformity. When resting length was decreased to 90% $L_{mt,r}$ finger extension was not achieved in any simulation (cf., Fig. 5, bottom row). Rather, substantial increases in passive flexion torques caused both MCP and PIP joints to remain flexed across all excitation levels.

In contrast to when $L_{mt,r}$ was modified, none of the simulations with the nominal "intrinsic-minus" model (3 simulations), increased joint laxity (9 simulations), or decreased extensor mechanical advantage (9 simulations) produced the claw finger deformity (Fig. 6). Notably, MCP hyperextension was a component of the final equilibrium position for each of these simulations, including our representation of acute intrinsic muscle paralysis without soft tissue changes (i.e., the "intrinsic-minus" model that incorporated nominal biomechanical properties; Fig. 6, top row). However, none of the final equilibrium positions included concurrent PIP flexion at the magnitude we defined as clawing.

The most severe deformities occurred within simulations that combined changes of all three of the variables of interest (Fig. 7). Like the results when $L_{mt,r}$ was decreased in isolation, the claw finger deformity was only present in the simulations that combined "mild" factors at 20% excitation and that combined "moderate" factors at 50% and 100% excitation (Fig. 7). Yet, in each case, the deformities were more severe. For example, the PIP joint was 35° more flexed (on average) in these three simulations compared to when only $L_{mt,r}$ was decreased.

Simulations of the Andre-Thomas compensation demonstrated the ability to reverse the claw finger deformity with wrist flexion (Fig. 8). Deformities that were present at 30° wrist extension were no longer present at 30° wrist flexion. Simulations that combined "severe" factors resulted in the deformity at 50% and 100% muscle excitation when the wrist was flexed.

4. DISCUSSION

To evaluate the effects of maladaptive changes in soft tissue biomechanical properties on the development and progression of the claw finger deformity following intrinsic muscle palsy, we completed 45 biomechanical simulations, varying muscle excitation level, clinically relevant biomechanical factors, and wrist position using a model of the "intrinsic-minus" hand. Contrary to our hypothesis, none of the simulations that increased joint laxity in isolation resulted in the claw finger deformity. Rather, of the mechanisms studied, shortening of the extrinsic finger flexors was the single factor most associated with the development of the claw finger deformity in simulation. The sensitivity of the claw finger deformity to even mild changes in extrinsic finger flexor muscle length was striking; a 2% decrease in resting length yielded the deformity while much more substantial changes in joint laxity and extensor moment arm (e.g., 75% decreases in the nominal parameters) did not. Notably, every simulation resulted in MCP hyperextension, including those completed

with our nominal model, which represented acute intrinsic muscle paralysis prior to any soft tissue changes. Thus, our simulations suggest that MCP hyperextension is primarily due to the absence of active intrinsic muscle function while the claw finger deformity only develops when biomechanical soft tissue property adaptations in the “intrinsic-minus” hand include shortening of the extrinsic finger flexors.

Further evidence of the sensitivity of the claw finger deformity to the length of the extrinsic finger flexor muscles is the reversal of the claw finger deformity with wrist flexion, clinically termed the Andre-Thomas sign. In the three cases where the claw finger deformity was present at 30° wrist extension (see Fig. 7), wrist flexion allowed PIP extension, reversing the deformity (see Fig. 8). As the wrist is flexed, the origins of the extrinsic finger flexor muscles are brought closer to the insertions, bringing these muscle-tendon lengths closer to $L_{mt,r}$. Thus, the passive resistive forces produced by the flexor muscles about the PIP joint are smaller at 30° wrist flexion than at 30° wrist extension, allowing the forces produced by the extensor muscles to extend the PIP joint. Therefore, the Andre-Thomas compensation likely takes advantage of the claw finger’s sensitivity to the passive resistive forces dictated by extrinsic flexor muscle length. Notably, this compensation strategy is often most successful acutely after intrinsic muscle paralysis and with mild claw finger deformities. However, as the deformity progresses the technique becomes less effective.[8,9] The sensitivity of this compensation strategy to increasing severity of the impairment is explainable by the fact that the passive resistive forces produced by extrinsic muscles become greater as the adaptive shortening of $L_{mt,r}$ becomes more severe, as we have simulated (see Fig. 4). Under these conditions, PIP extension and the reversal of the deformity are limited, even at flexed wrist positions (see Fig. 5, 7, and 8, severe conditions)

Because our results contradicted our initial hypothesis that increased joint laxity would be the factor most likely to generate the claw finger deformity, we evaluated potential biases in our simulation analysis. One potential source of bias is that we simulated a uniform increase in joint laxity across all three finger joints. If changes in joint laxity occur heterogeneously at the MCP, PIP, and DIP, the force balance between joints as well as the coordination and timing of finger extension could be affected. However, development of the claw finger deformity requires a net passive flexion torque in flexed positions, large enough to prevent the extensor muscles from extending the PIP and DIP joints. Increased laxity of the three finger joints, whether uniform or heterogeneous, decreases the flexion torques about these joints. A second potential bias of our model is that we did not explicitly include the extensor mechanism and its complex network of force transmission to the distal segments of the fingers. Rather, we modeled the passive properties of the intrinsic muscles and other soft tissues within the hand as torsional spring-dampers that act independently about each joint. The intrinsic finger muscles act across the MCP, PIP, and DIP joints via the extensor mechanism. Thus, our simulations do not couple passive flexion torques produced by the intrinsic muscles at the MCP with passive extension torques at the IP joints. Including these coupled torques would have decreased the severity of the claw finger deformity we simulated because additional passive IP extension torques would have been added during MCP hyperextension. Similarly, biomechanical changes following paralysis of the intrinsic muscles that may increase the muscles’ passive stiffness were not included in our model, but would likely further decrease the severity of the deformity, through the coupling actions of

the extensor mechanism.[36,37] Thus, despite limitations and potential biases associated with our modeling choices, none of these biases would contradict our conclusion that the deformity is most sensitive to changes in the lengths of the extrinsic flexor muscles. Especially because of the lack of quantitative data describing passive biomechanical joint properties in the hand, experimental paradigms that test our modeling assumptions would benefit the field.

This simulation study provides data that suggest the development and progression of the claw finger deformity is extremely sensitive to shortening, or contracture, of extrinsic finger flexors in simulation. These findings are consistent with previous work that has demonstrated finger flexion contractures correlate with poor outcomes following surgical inventions within the intrinsic minus hand.[38] Thus, maintaining the length of the extrinsic finger flexors, via stretching and splinting, should be an area of focus of rehabilitation. The goal of such interventions would be to prevent or delay the development of the claw finger deformity in both the acute and chronic stages of intrinsic finger paralysis, and for surgical candidates to achieve optimal outcomes following surgery.

Acknowledgements

This work was supported by a Promotion of Doctoral Studies (PODS) – Level II Scholarship from the Foundation for Physical Therapy, American Heart Association – Pre-Doctoral Fellowship: 16PRE30970010, & NIH R01HD084009 Dewald/Murray (PIs)

REFERENCES

1. Kozin SH, Porter S, Clark P, Thoder JJ. The contribution of the intrinsic muscles to grip and pinch strength. J Hand Surg Am. 1999;24(1):64–72. [PubMed: 10048518]
2. Li ZM, Zatsiorsky VM, Latash ML. Contribution of the extrinsic and intrinsic hand muscles to the moments in finger joints. Clin Biomech (Bristol, Avon). 2000;15(3):203–211.
3. Darling WG, Cole KJ. Muscle activation patterns and kinetics of human index finger movements. J Neurophysiol. 1990;63(5):1098–1108. [PubMed: 2358864]
4. Srinivasan H Patterns of movement of totally intrinsic-minus fingers based on a study of one hundred and forty-one fingers. J Bone Joint Surg Am. 1976;58(6):777–785. [PubMed: 956222]
5. Palti R, Vigler M. Anatomy and function of lumbrical muscles. Hand Clin. 2012;28(1):13–17. [PubMed: 22117920]
6. Brand PW. Paralytic claw hand; with special reference to paralysis in leprosy and treatment by the sublimis transfer of Stiles and Bunnell. J Bone Joint Surg Br. 1958;40-B(4):618–632. [PubMed: 13610974]
7. Brand PW, Hollister A. Clinical mechanics of the hand. 2nd ed. St. Louis: Mosby Year Book; 1993.
8. Sapienza A, Green S. Correction of the claw hand. Hand Clin. 2012;28(1):53–66. [PubMed: 22117924]
9. Schreuders TAR, Brandsma JW, Stam HJ. The intrinsic muscles of the hand - Function, assessment and principles for therapeutic intervention. Physikalische Medizin Rehabilitationsmedizin Kurortmedizin. 2007;17(1):20–27.
10. Zancolli EA. Claw-hand caused by paralysis of the intrinsic muscles: a simple surgical procedure for its correction. J Bone Joint Surg Am. 1957;39-A(5):1076–1080. [PubMed: 13475406]
11. Tabary JC, Tabary C, Tardieu C, Tardieu G, Goldspink G. Physiological and structural changes in the cat's soleus muscle due to immobilization at different lengths by plaster casts. J Physiol. 1972;224(1):231–244. [PubMed: 5039983]
12. Williams PE, Goldspink G. Changes in sarcomere length and physiological properties in immobilized muscle. J Anat. 1978;127(Pt 3):459–468. [PubMed: 744744]

13. Colditz J Splinting the Hand with a Peripheral-Nerve Injury In: Mackin Callahan, Osterman Skirven, Schneider Hunter, eds. Rehabilitation of the Hand and Upper Extremity. 5th ed: Mosby; 2002:622–634.
14. Sousa GGQ, de Macedo MP. Effects of a dynamic orthosis in an individual with claw deformity. Journal of Hand Therapy. 2015;28(4):425–428. [PubMed: 26190028]
15. Chan RK. Splinting for peripheral nerve injury in upper limb. Hand Surg. 2002;7(2):251–259. [PubMed: 12596288]
16. Mikhail IK. Bone Block Operation for Clawhand. Surg Gynecol Obstet. 1964;118:1077–1079. [PubMed: 14143460]
17. Riordan DC. Tendon transplantations in median-nerve and ulnar-nerve paralysis. J Bone Joint Surg Am. 1953;35-A(2):312–320; passim. [PubMed: 13052603]
18. Srinivasan H The extensor diversion graft operation for correction of intrinsic minus fingers in leprosy. J Bone Joint Surg Br. 1973;55(1):58–65. [PubMed: 4693893]
19. Smith RJ. Metacarpal ligament sling tenodesis. Bull Hosp Jt Dis Orthop Inst. 1984;44(2):466–469. [PubMed: 6099189]
20. Littler JW. Tendon transfers and arthrodeses in combined median and ulnar nerve paralysis. J Bone Joint Surg Am. 1949;31A(2):225–234. [PubMed: 18116560]
21. Taylor NL, Raj AD, Dick HM, Solomon S. The correction of ulnar claw fingers: A follow-up study comparing the extensor-to-flexor with the palmaris longus 4-tailed tendon transfer in patients with leprosy. Journal of Hand Surgery-American Volume. 2004;29a(4):595–604.
22. Bunnell S Surgery of the intrinsic muscles of the hand other than those producing opposition of the thumb. Journal of Bone and Joint Surgery. 1942;24:1–31.
23. Binder-Markey BI, Murray WM. Incorporating the length-dependent passive-force generating muscle properties of the extrinsic finger muscles into a wrist and finger biomechanical musculoskeletal model. J Biomech. 2017;61:250–257. [PubMed: 28774467]
24. Delp SL, Anderson FC, Arnold AS, et al. OpenSim: open-source software to create and analyze dynamic simulations of movement. IEEE Trans Biomed Eng. 2007;54(11):1940–1950. [PubMed: 18018689]
25. Zajac FE. Muscle and tendon: properties, models, scaling, and application to biomechanics and motor control. Crit Rev Biomed Eng. 1989;17(4):359–411. [PubMed: 2676342]
26. Hogg RV, Ledolter J. Engineering statistics New York, London: Collier Macmillan; 1987.
27. Le Minor JM, Rapp E. Relative weights of the human carpal bones: biological and functional interests. Ann Anat. 2001;183(6):537–543. [PubMed: 11766525]
28. McConville JT, Churchill TD, Kaleps I, Clauser CE, Cuzzi J. Anthropometric Relationships of Body and Body Segment Moments of Inertia. Anthropology Research Project. 1980;AFAMRL-TR-80–119.
29. Blana D, Chadwick EK, van den Bogert AJ, Murray WM. Real-time simulation of hand motion for prosthesis control. Comput Methods Biomech Biomed Engin. 2017;20(5):540–549. [PubMed: 27868425]
30. Darling WG, Cole KJ, Miller GF. Coordination of index finger movements. J Biomech. 1994;27(4):479–491. [PubMed: 8188728]
31. de los Reyes-Guzman A, Gil-Agudo A, Penasco-Martin B, Solis-Mozos M, del Ama-Espinosa A, Perez-Rizo E. Kinematic analysis of the daily activity of drinking from a glass in a population with cervical spinal cord injury. J Neuroeng Rehabil. 2010;7:41. [PubMed: 20727139]
32. Reghem E, Cheze L, Coppens Y, Pouydebat E. The influence of body posture on the kinematics of prehension in humans and gorillas (Gorilla gorilla). Exp Brain Res. 2014;232(3):1047–1056. [PubMed: 24430026]
33. Ryu JY, Cooney WP 3rd, Askew LJ, An KN, Chao EY. Functional ranges of motion of the wrist joint. J Hand Surg Am. 1991;16(3):409–419. [PubMed: 1861019]
34. Knutson JS, Kilgore KL, Mansour JM, Crago PE. Intrinsic and extrinsic contributions to the passive moment at the metacarpophalangeal joint. J Biomech. 2000;33(12):1675–1681. [PubMed: 11006392]

35. Kamper DG, Hornby GT, Rymer WZ. Extrinsic flexor muscles generate concurrent flexion of all three finger joints. J Biomech. 2002;35(12):1581–1589. [PubMed: 12445611]

36. Sato EJ, Killian ML, Choi AJ, et al. Skeletal muscle fibrosis and stiffness increase after rotator cuff tendon injury and neuromuscular compromise in a rat model. J Orthop Res. 2014;32(9):1111–1116. [PubMed: 24838823]

37. Nikolaou S, Hu L, Cornwall R. Afferent Innervation, Muscle Spindles, and Contractures Following Neonatal Brachial Plexus Injury in a Mouse Model. J Hand Surg Am. 2015;40(10):2007–2016. [PubMed: 26319770]

38. Ebenezer M, Rao K, Partheebarajan S. Factors affecting functional outcome of surgical correction of claw hand in leprosy. Indian J Lepr. 2012;84(4):259–264. [PubMed: 23720890]

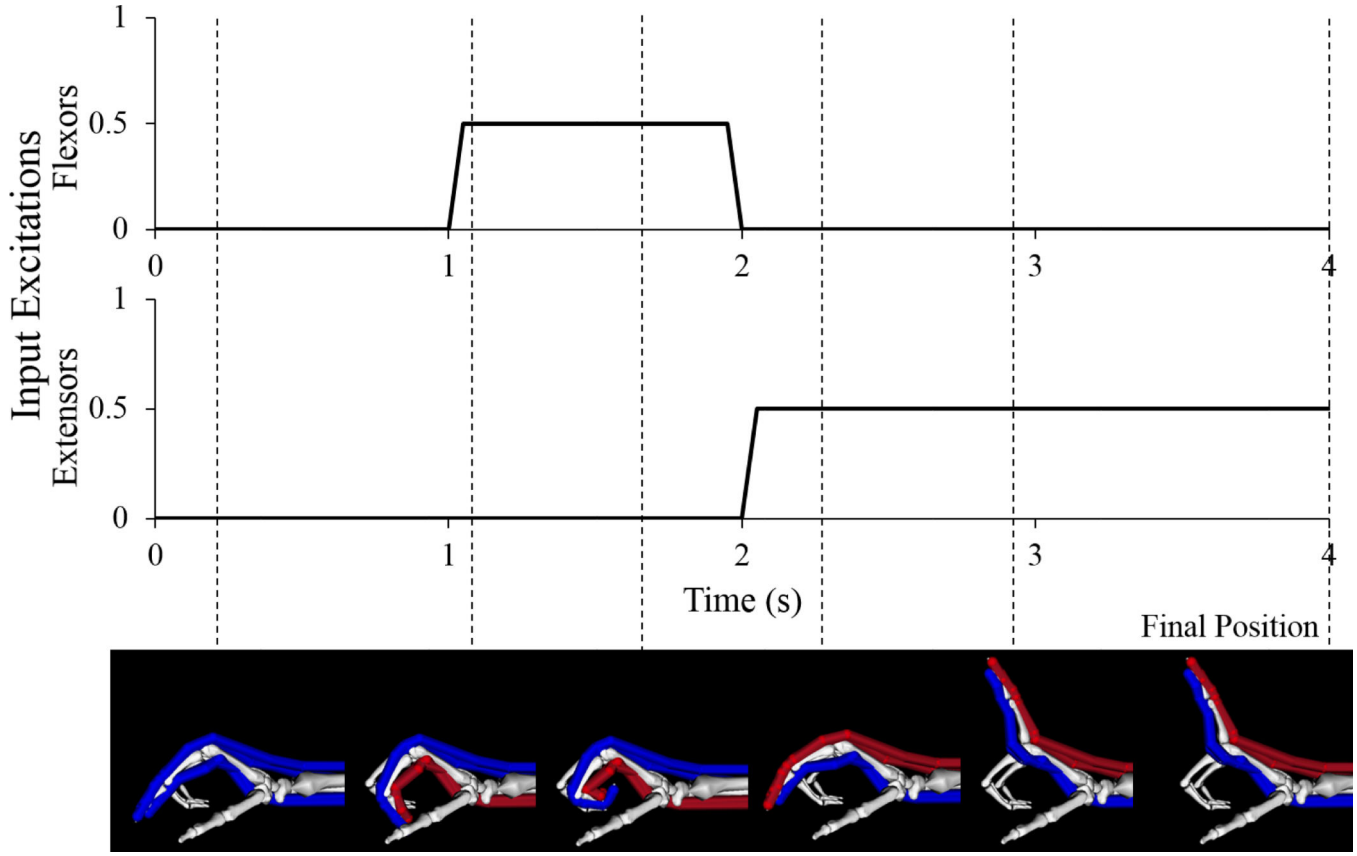

Figure 1:

Excitation inputs and resulting index finger motion for one of the four second forward dynamic simulations completed in this study (nominal model, 50% excitation level). Uniform excitation inputs were defined for the two extrinsic flexors of the index finger and the two extrinsic extensors. In these images, muscle-tendon paths that are blue indicate the muscles are passive, or “off” (0% excitation); paths that are red indicate the muscles are active, or “on” (50% excitation in this example). Dashed lines indicate the time at which the index finger reached the pictured position during the simulation, final dashed line indicates the final position used for the determination of the claw finger deformity.

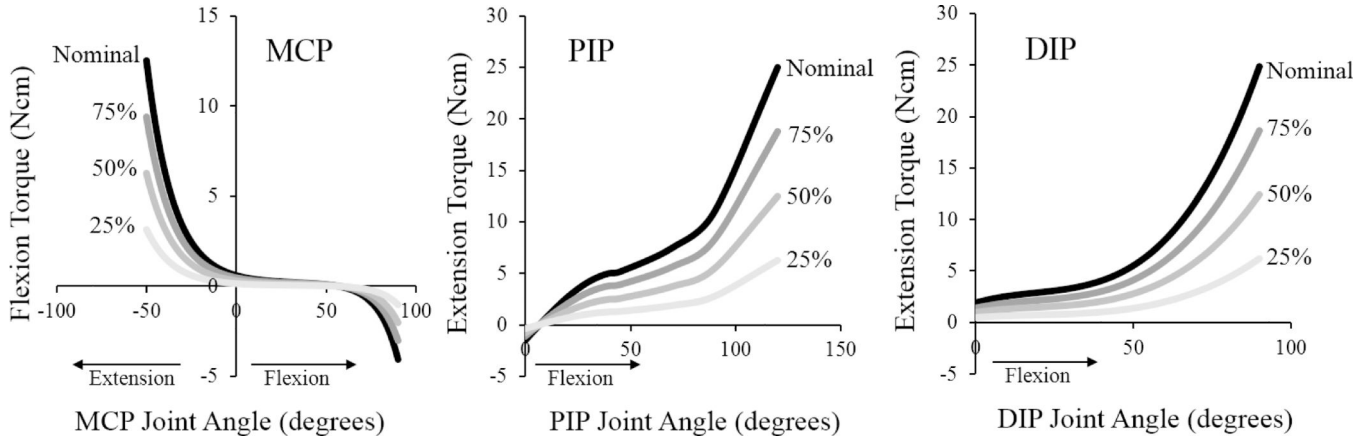

Figure 2:

Passive torques defined in the “intrinsic-minus” model, including the passive elastic torques produced by intrinsic muscles and joint structures in the nominal model (black) and torques scaled to simulate increased joint laxity. For a given simulation with increased laxity, the torques in the nominal model were scaled to one of three different magnitudes (shades of grey).

Uniform scaling was implemented across the MCP, PIP, and DIP joints in a given simulation.

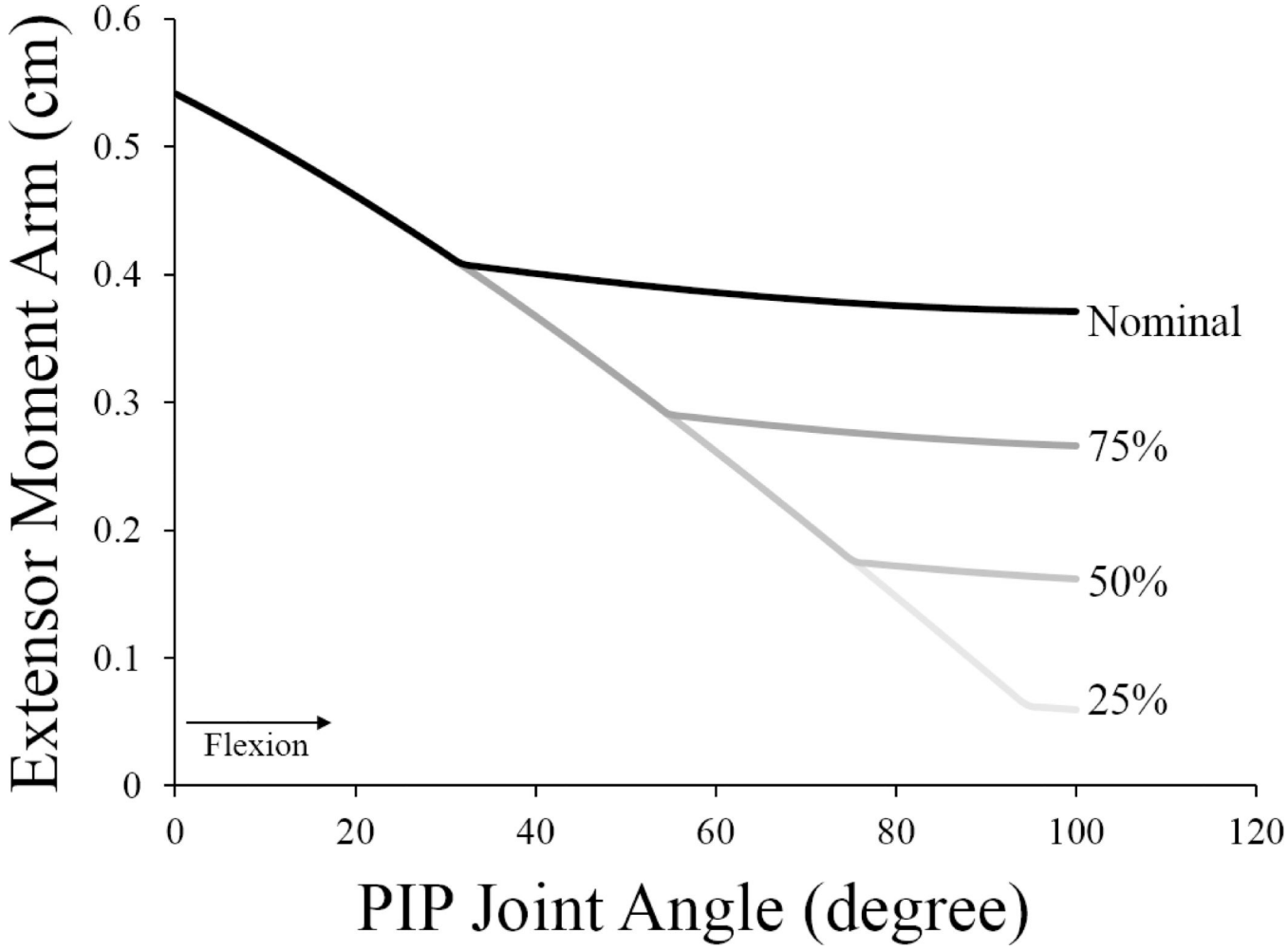

Figure 3:

Extensor moment arm of the extrinsic extensors at the PIP joint as a function of PIP joint angle. The black line indicates the moment arm of the nominal model; grey lines indicate the moment arms for the models where the diameter of the joint kinematic constraint was decreased to simulate volar translation of the lateral slips of the extensor mechanism. In all models, the moment arms of the EDCI and EIP are identical. The kinematic constraint is a part of the model of the geometry of the joint. Note that in full extension (0° PIP flexion), the muscle-tendon path is initially not in contact with the joint. All simulations have the same moment arms until the muscle-tendon path reaches the kinematic constraint, at which point the moment arm of that model diverges because the muscle-tendon path wraps over its surface. As the diameter of the constraint is decreased, the muscle-tendon path moves closer to joint center of rotation before making contact, decreasing the moment arms of the extensor muscles about the joint.

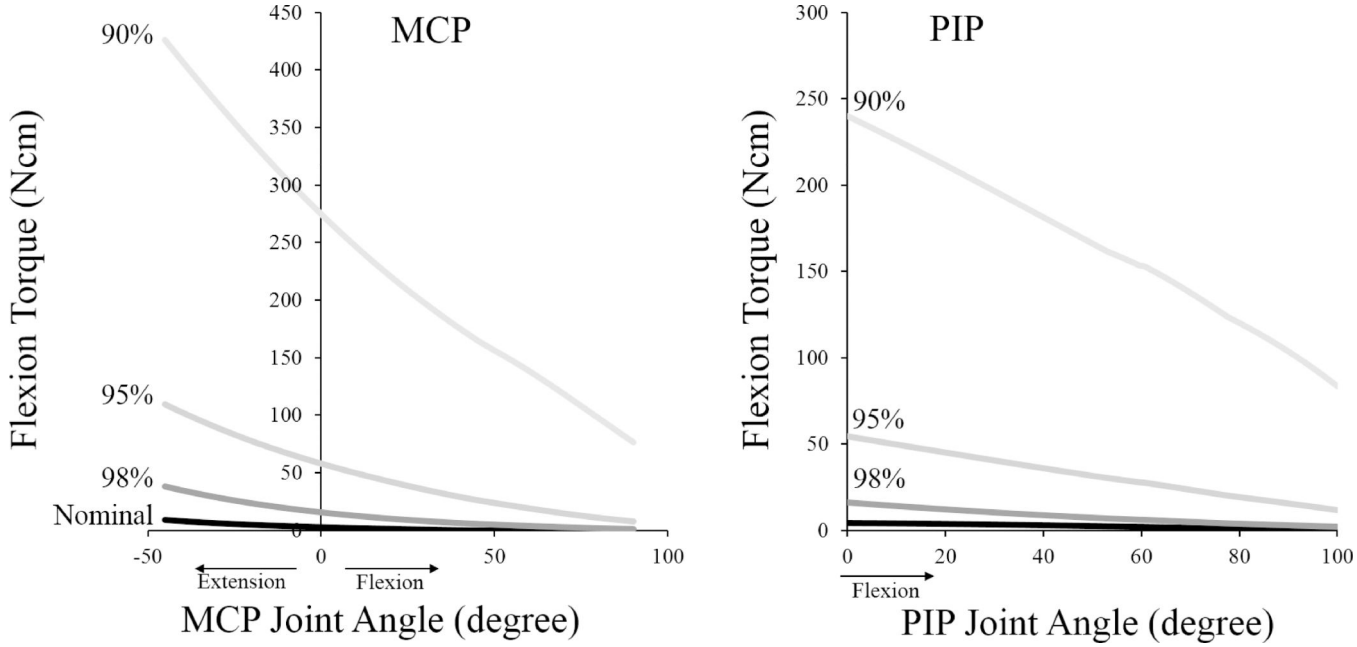

Figure 4:

Net passive flexion torque about the MCP (left) and PIP (right) joints generated by the extrinsic flexor muscles of the index finger, as a function of joint angle. The black line (in both plots) indicates the net torque produced by these two muscles in the nominal model. Grey lines indicate the net passive torques generated when the resting lengths of both muscles were shortened to 98%, 95%, and 90% of their lengths (shades of grey). Positive angles indicate flexion, negative angles indicate extension.

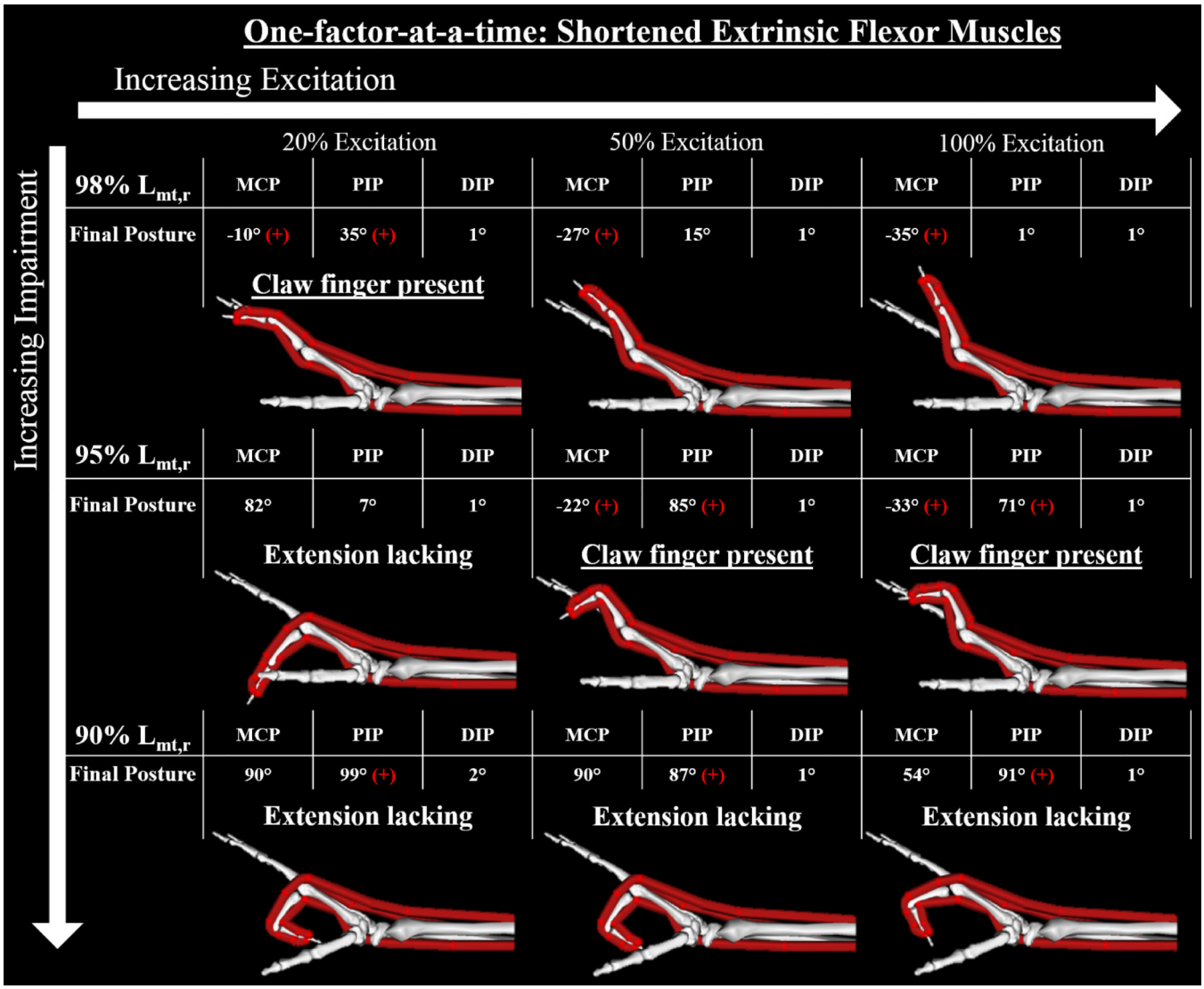

Figure 5:

Final equilibrium positions of the 9 forward simulations with shortened flexor muscles. Claw finger deformity was defined to be present when the final position included both hyperextension (extension beyond 0 degrees) of the MCP joint and concurrent flexion of the PIP joint greater than 20 degrees. In this figure, a red "+" indicates when either of these two conditions was present in a single simulation. The simulation results indicate that the deformity is sensitive to both impairment level and muscle excitation. Specifically, mild changes (98% $L_{mt,r}$) yielded the claw finger deformity at low excitation levels, but finger extension was achieved with higher excitations (top row). In contrast, coordinated finger extension was not achievable at any excitation level following moderate (95% $L_{mt,r}$) and severe (95% $L_{mt,r}$) changes (middle and bottom rows).

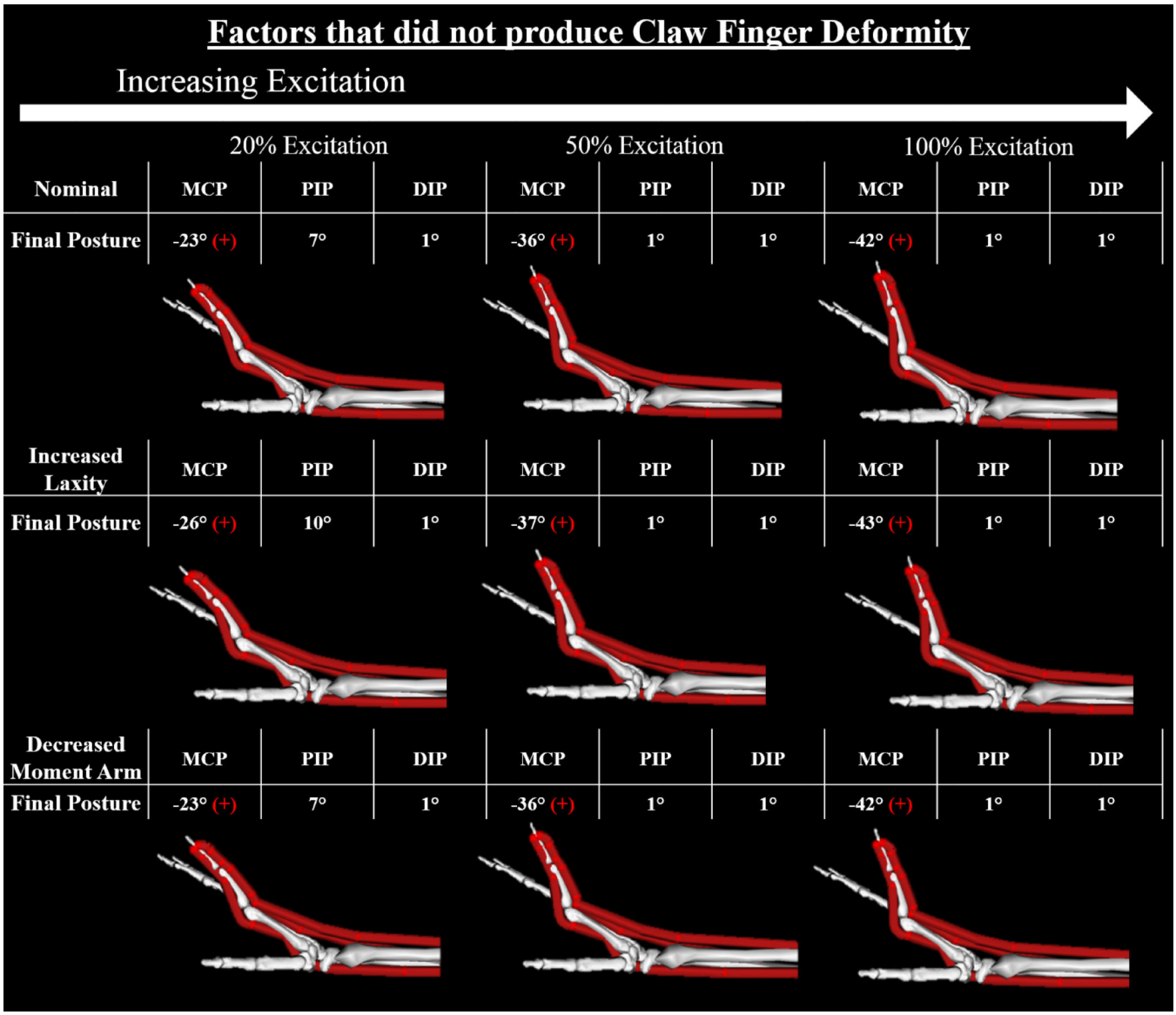

Figure 6:

Final equilibrium positions for the 3 simulations involving the nominal “intrinsic-minus’ model, the 3 simulations involving moderate changes to joint laxity (50% nominal torque), and the 3 simulations involving moderate changes to PIP extensor moment arm (50% decrease in the radius of the kinematic constraint). Claw finger deformity was defined to be present when the final position included both hyperextension (extension beyond 0 degrees) of the MCP joint and concurrent flexion of the PIP joint greater than 20 degrees. In this figure, a red “+” indicates when either of these two conditions was present in a single simulation. Under these conditions, all impairment and excitation levels demonstrated hyperextension of the MCP joint. None of the nominal simulations and none of those that involved isolated changes to joint laxity or PIP extensor moment arm resulted in a claw finger deformity. Results for the 3 mild and 3 severe simulations for these two factors not shown, due to their similarity to the moderate results.

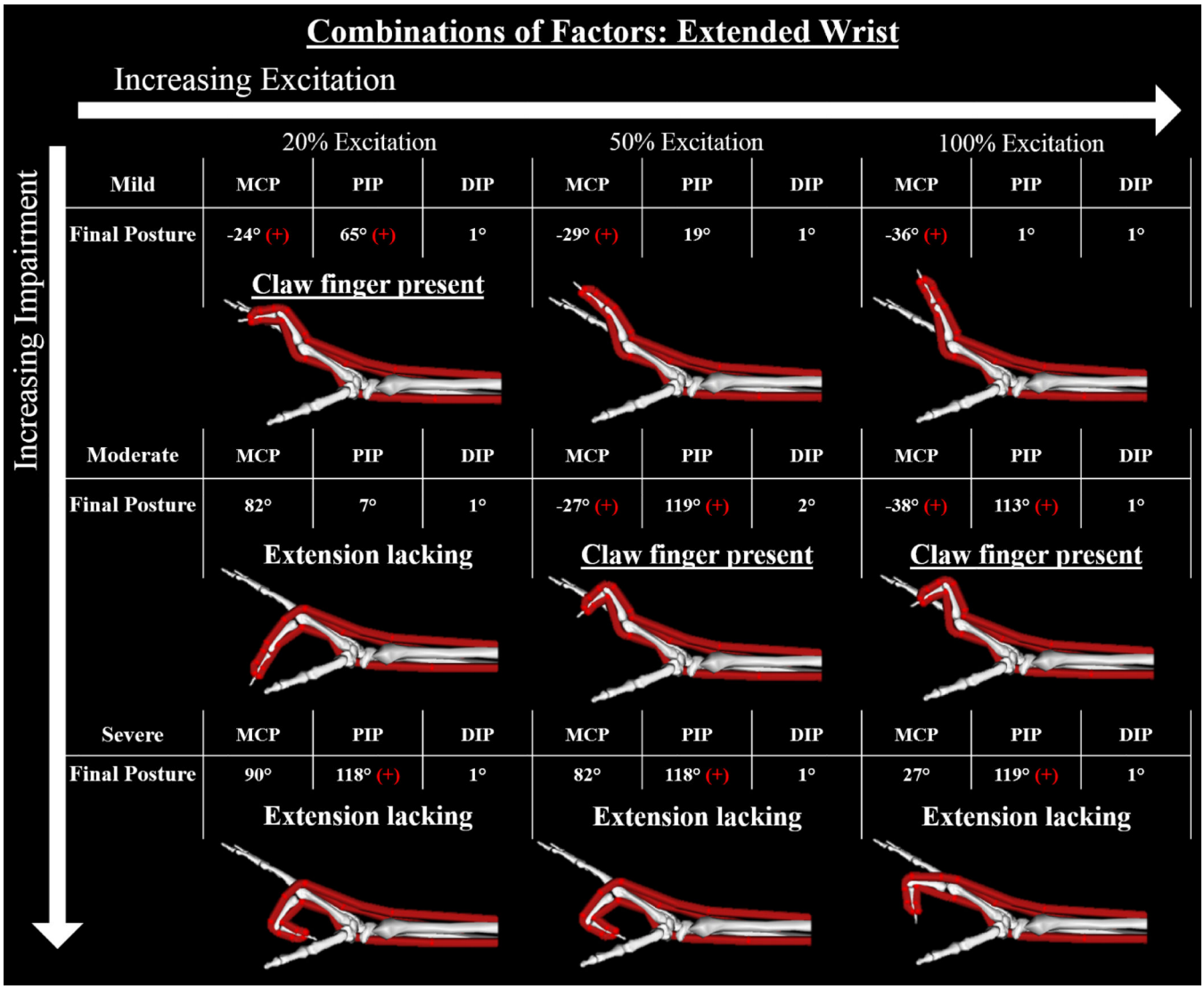

Figure 7:

Final equilibrium positions for the 9 forward simulations in which the multiple factors were combined simultaneously. Red "+" indicates that either the MCP is hyperextended or the PIP is flexed more than 20 degrees, positive for both indicates the claw finger deformity. The most severe claw finger deformities occurred within simulations that combined changes of all three of the variables of interest. The presence of the claw finger deformity mimics that observed when $L_{mt,r}$ was shortened in isolation (see Fig 5), although the resulting deformities were more severe when changes to the three biomechanical factors were combined.

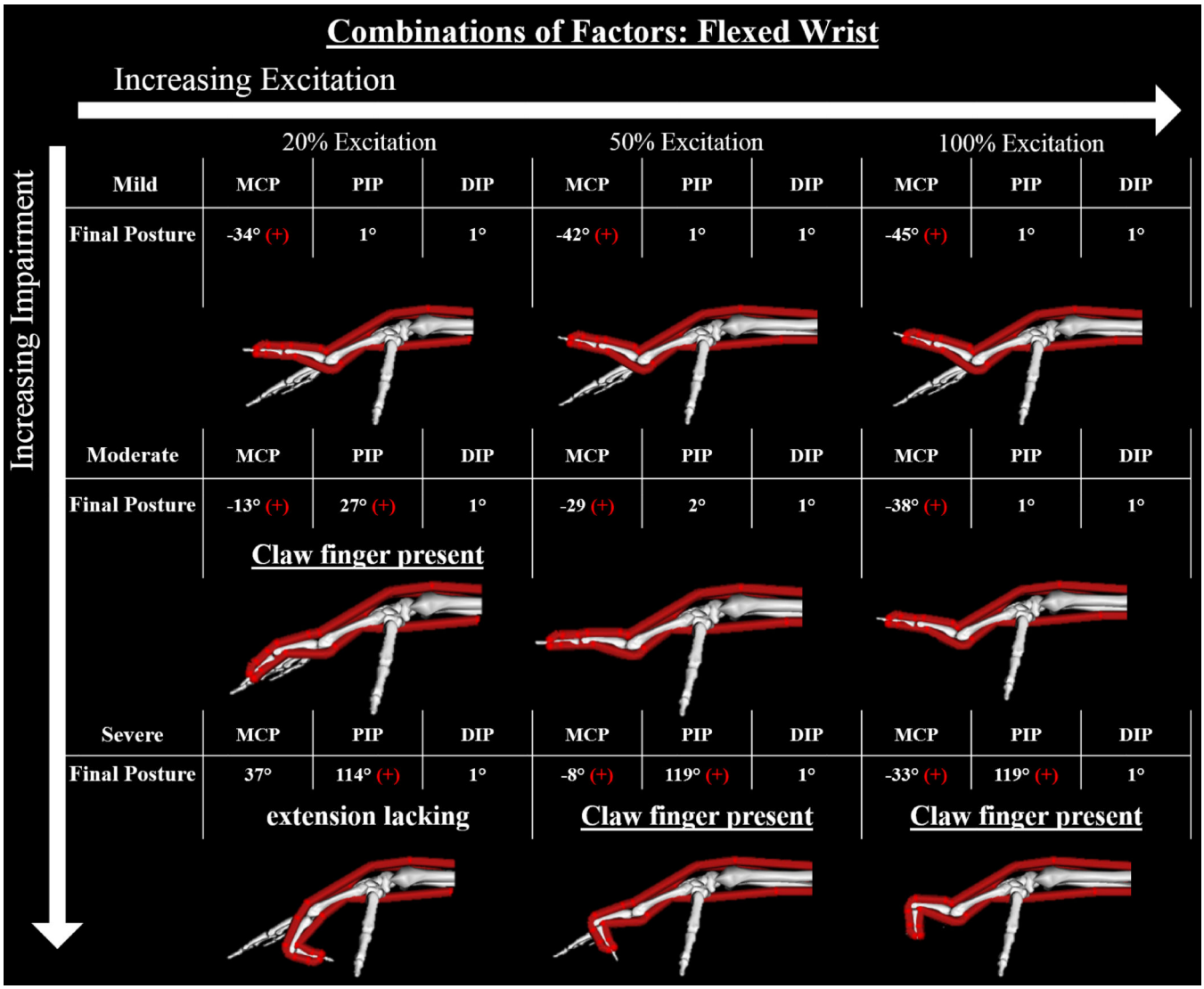

Figure 8:

Final equilibrium positions for the 9 forward simulations of the models combining the mild, moderate, and severe changes and a flexed wrist. Red "+" indicates either the MCP is hyperextended or the PIP is flexed more than 20 degrees, positive for both indicates the claw finger deformity. As the wrist is flexed the muscle-tendon lengths of the extrinsic finger flexors shorten to lengths closer to $L_{mt,r}$. Thus, the passive resistive forces produced by the flexor muscles about the PIP joint are smaller at 30° wrist flexion than at 30° wrist extension, allowing the forces produced by the extensor muscles to be more effective.

Table 1:

Summary of the simulations run during the sensitivity analysis.

		Wrist extended 30°												Wrist flexed 30°		
		"One-factor-at-a-time"									Combined			Combined		
	Nominal Model	Increased Laxity			Decreased Moment Arm			Shortened Flexors			Mild	Moderate	Severe	Mild	Moderate	Severe
		75% nominal	50% nominal	25% nominal	75% nominal	50% nominal	25% nominal	98% nominal	95% nominal	90% nominal						
Input	20%	20%	20%	20%	20%	20%	20%	20%	20%	20%	20%	20%	20%	20%	20%	20%
	50%	50%	50%	50%	50%	50%	50%	50%	50%	50%	50%	50%	50%	50%	50%	50%
	100%	100%	100%	100%	100%	100%	100%	100%	100%	100%	100%	100%	100%	100%	100%	100%
N	3			9			9			9			9			9

Table 2:

Muscle parameters at nominal lengths and shortened to 98%, 95%, and 90% of nominal length.

		Nominal	98%	95%	90%
FDSI	Optimal Fiber Length (m)	0.0835	0.0818	0.0793	0.0752
	Tendon Slack Length (m)	0.2772	0.2717	0.2633	0.2495
	Pennation Angle	6°	6°	6°	6°
	Resting Muscle-Tendon Length (m)	0.3602	0.3531	0.3422	0.3243
FDPI	Optimal Fiber Length (m)	0.0749	0.0734	0.0712	0.0674
	Tendon Slack Length (m)	0.3044	0.2983	0.2892	0.274
	Pennation Angle	7°	7°	7°	7°
	Resting Muscle-Tendon Length (m)	0.3787	0.3712	0.3599	0.3409
Resting finger position at 30° wrist extension	MCP (deg)	71°	83°	90°	90°
	PIP (deg)	7°	12°	34°	99°
	DIP (deg)	2°	2°	2°	43°